SEMARAK ILMU PUBLISHING

Advances in Fluid, Heat and Materials Engineering

Journal homepage:
https://semarakilmu.com.my/journals/index.php/afhme/index
ISSN: 3083-8134

Computational Analysis of Temperature Distributions on the Malignant Tumour

Khairul Shafaiz Bin Jesni[1], Ishkrizat Taib[1,*]

[1] Faculty of Mechanical and Manufacturing Engineering, Universiti Tun Hussein Onn Malaysia, 86400 Parit Raja, Batu Pahat, Johor, Malaysia

ARTICLE INFO

Article history:
Received 1 October 2024
Received in revised form 14 October 2024
Accepted 5 November 2024
Available online 31 December 2024

Keywords:
Tumor; breast cancer; heat propagation

ABSTRACT

Breast cancer is a critical illness in Malaysia, as shown in the statistical data listed by the National Institute of Cancer. Typically, the patient undergoes lumpectomy or mastectomy, followed by chemotherapy and radiotherapy. However, patients experience side effects after treatment. Based on our previous findings, heating the body from 40°C to 44°C is an alternative treatment to reduce the side effects of this medical treatment. Thus, this study investigated heat propagation in malignant tumours of different sizes. Three different breast tumour models with different sizes were created. The heat propagation was simulated using the computational fluid dynamics (CFD) method. Three different temperatures were applied to malignant tumours exposed to infrared sources. From the observations, model 2 mm showed the highest temperature propagation compared to the others. Heat propagation in blood vessels also exerts a significant radiation effect, as observed in tumours. However, the velocity and pressure of blood vessels did not significantly change in the models. In conclusion, heat propagation via infrared sources managed to penetrate tumours, and early-stage tumours experienced better heat propagation compared to others.

1. Introduction

One of the most dangerous diseases worldwide is tumours [1,2]. Tumours can grow at any part of the body either inside organ like brain and lungs, or on outer organs, such as organs [3]. In the first stage, the condition is not cancerous because the condition can still be controlled. However, as a tumor grows and spreads throughout the body, it becomes cancerous [4-6]. If the patient does not receive appropriate treatment quickly, the risk of mortality is high. Therefore, cancer treatment is necessary to eliminate cell tumors before they spread widely [7].

For many years, electromagnetic radiation has been used in medical treatment [8]. X-rays, magnetic resonance imaging, and lasers are used to treat diseases [9-11]. This has shown that it has successfully treated many people worldwide. Different types of cancer treatment, such as surgery, radiation therapy, and chemotherapy, are available.However, these treatments can have several side

* *Corresponding author.*
E-mail address: iszat@uthm.edu.my

https://doi.org/10.37934/afhme.3.1.1021

effects, which can be temporary or permanent. Hyperthermia is a treatment that can be considered. This technique neglects the use of chemicals or harmful radiation [12-15].

It is important to conduct simulations before applying the proposed treatment method. This will ensure that treatment has a high possibility of causing cancer. The simulation can provide an accurate estimation of the radiation effect on the tumour tissue. There are many ways to perform simulations. One way to perform the simulation is to use the computational fluid dynamics method.

Computational fluid dynamics (CFD) tools are used in the engineering field, especially when they are involved in the design and analysis. CFD has become one of the primary methods used by bioengineers to simulate the flow properties in desired objects. Computer modeling makes a significant contribution to the field and is a significant tool for studying different tumor sizes. Detailed statistical data distribution was promoted in this study to determine the physical changes and heat distribution in different tumor sizes to enable analysis of the effect of infrared radiation on malignant tumors.

Tumors are masses or lumps of tissue that may resemble swelling [16-19]. It develops when cells reproduce quickly. Some tumors are noncancerous. However, malignant tumour is tumour that cancerous. It is important to receive appropriate treatment before disease spreads. There are many treatments for it, such as surgery, radiation therapy, and chemotherapy. Available treatments manage cancer treatment, but they come at a cost. In this study, a simulation was created to determine how infrared radiation affects malignant tumors and prevent their spread. Different sizes of tumor tissue models will be created to obtain better results. The simulation was performed using CFD software due to its ability to reveal changes in the physical properties of the model.

The aim of this study was to identify malignant tumors that have taken a long time to live. Before selecting the topic, identifying the problems encountered by the surroundings is the initial step that requires detailed investigation. This study investigated the effects of malignant tumors in humans and the effectiveness of current treatments. Next, changing the treatment method using electromagnetic pulses will have some effect, for example, on the surface of the tumour.

2. Methodology

2.1 Flow Chart

Figure 1 presents a step-by-step numerical simulation approach for studying heat conduction in malignant tumors. This section begins with a problem statement and a literature review of the impact of electromagnetic fields on tumor. Subsequently, the geometry of the tumor was developed for simulation, and the simulation parameters were decided. The heat propagation was then simulated, validation follows next. If the results are not validated, the simulation parameters are changed, and the process is repeated. After validation, the results were discussed in terms of heat distribution, and the study concluded with recommendations.

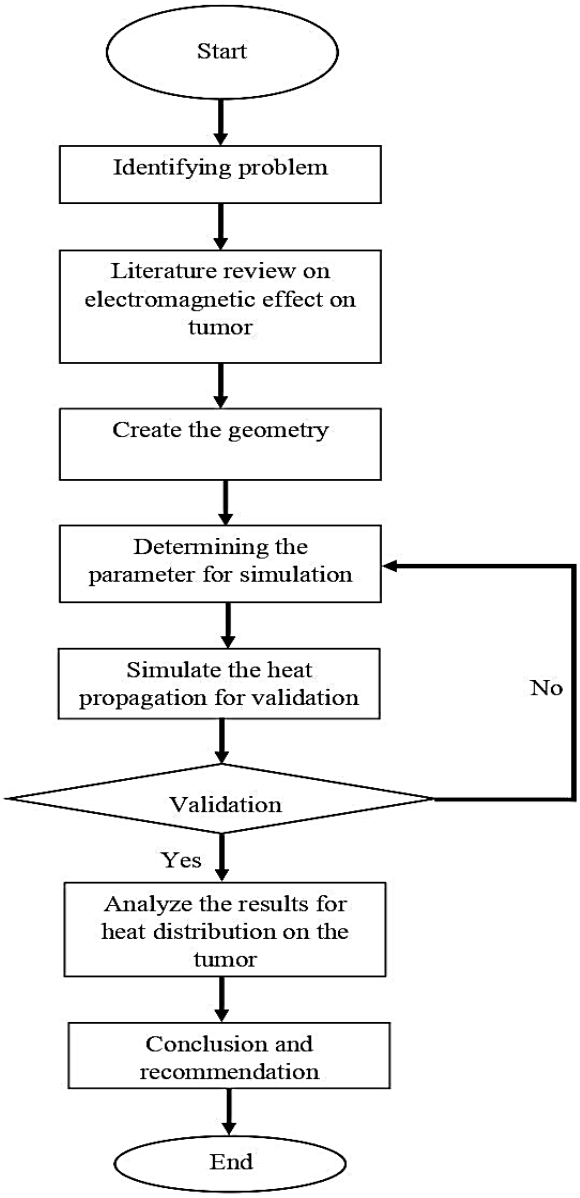

Fig. 1. Flow chart of modelling on the malignant tumor

2.2 Discretization Technique

In this study, the finite volume method was applied. Because heat flux is a type of flux study, the heat penetration formula, heat radiation equation, and Pennes' bioheat equation are suitable as governing equations.

2.2.1 Heat penetration equation

The heat-penetration equation is typically used to calculate the heat-penetration factors of liquid and solid foods. Because tumor tissues are in a solid state, it is not problematic to examine this theory. Heat penetration factor, f_h formula for solid.

$$fh = \frac{2.3 \times C\rho \times \rho}{k \times S^2} \quad (1)$$

where, Cρ is specific heat capacity, ρ is density and k is thermal conductivity.

2.2.2 Heat radiation equation

There are three types of heat transfers: heat conduction, heat convection, and heat radiation. Because electromagnetic radiation is a type of radiation, heat radiation was used in this study to calculate the rate of heat transfer in the tumour tissue. The general formula for heat radiation is based on the Stefan-Boltzmann:

$$\frac{Q}{t} = \sigma e A T^4 \tag{2}$$

where:
σ = 5.67 × 10^{-8} J/s · m^2 · K^4 (Stefan-Boltzmann constant)
A = surface area of the object
T = absolute temperature in kelvin
e = emissivity

2.2.3 Pennes bioheat equation

The Pennes bioheat equation is the most suitable mathematical model used in this study. It was developed by Chanmugam *et al.,* [20] used this equation to model heat transfer in breast tissue. The Pennes bioheat equation is given by:

$$\rho c \frac{\partial T}{\partial t} = k\nabla^2 T + \rho_b c_b \omega_b (T_a - T) Q_m \tag{3}$$

where:
ρ = tissue density (kg/m³)
c = specific heat of the tissue (J/kg·K)
T = temperature (°C or K)
t = time (s)
k = thermal conductivity of the tissue (W/m·K)
ρ_b = blood density (kg/m³)
c_b = specific heat of blood (J/kg·K)
ω_b = blood perfusion rate (1/s)
T_a = arterial blood temperature (°C or K)
Q_m = metabolic heat generation (W/m³)

2.3 Meshing

A computational mesh was generated tumour model using the ANSYS Meshing application after the model was constructed. Misalignment of mesh faces causes errors and smears the result because mesh alignment with the flow is important. The proposed method reduces mesh cell counts while maintaining solution accuracy. The basic parameters were set and adjusted for meshing to obtain finer meshes. Mesh structure errors are a common problem that lead to simulation failure. This could be because the mesh was too coarse and did not cover all single element cells individually; rather,

several effects changed when the mesh became finer. For this model, a tetrahedral mesh was selected for the simulation.

2.4 Parameter Assumption

The dimensions of the model were decided by considering relevant values based on previous studies. The radius of the tumours will be the manipulation variable. Table 1 lists the results of the determined values for the model dimensions. Figure 2 shows the schematic of tissue layers, including the epidermis, fat, blood vessels, and tumor and its dimension.

Table 1
The parameter of the model

Parameter	Dimension (mm)
Radius of the epidermis	5.5
Radius of the fat layer	5
Radius of blood vessel	0.5
Length of blood vessel	18
Radius of the tumor	2, 3, and 4

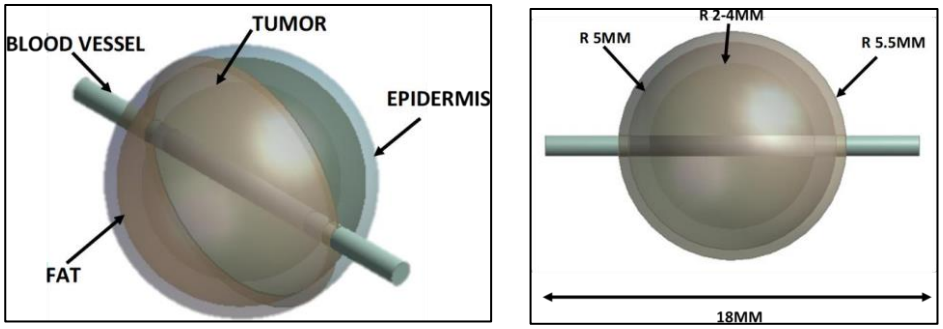

(a) (b)

Fig. 2. Tumor model (a) Labeled model (b) Dimension

2.5 Simplified Tumour Model

The three-dimensional geometry of the simplified tumour model was based on a previous study. It consists of four main parts : the epidermis, fat, tumour, and blood vessel. The tissue was spherical, whereas the blood vessel was cylindrical. The models were generated using a commercially aided design software called Design Modeler as shown in Figure 3. The 4-mm tumor was labeled Model A, followed by Model B for the 3-mm tumour and Model C for the 2-mm tumour.

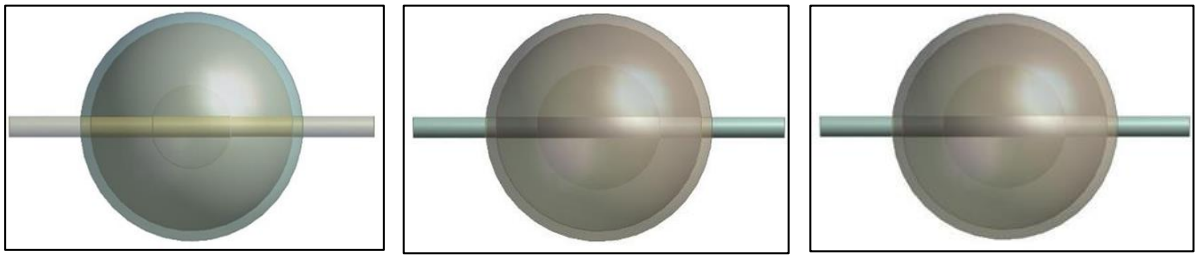

(a) (b) (c)

Fig. 3. Tumor model (a) A = 4 mm (b) B = 3 mm (c) C = 2 mm

2.6 Boundary Condition

For this study, the types of parameters that were set as the boundary conditions were density, thickness, and specific heat capacity. Table 2 lists the boundary condition values based on a previous study.

Table 2
Model parameters

Boundary condition	Value
Density of the epidermis	1200 kg/m^3
Density of the tumor	1050 kg/m^3
Density of fat	930 kg/m^3
Density of blood	1060 kg/m^3
Thickness of fat layer in the tumor	1 mm
Thickness of the epidermis in the tumor	0.5 mm
Specific heat capacity of the tumor	3852 J/kgK
Specific heat capacity of the epidermis	3589 J/kgK
Specific heat capacity of fat	2770 J/kgK
Specific heat capacity of blood	3770 J/kgK
Blood viscosity	0.0049 Ns/m^2
Thermal conductivity of the epidermis	0.35 W/mK
Thermal conductivity of fat	0.25 W/mK
Thermal conductivity of tumor	0.5 W/mK
Thermal conductivity of blood	0.52 W/mK
Velocity of blood	0.049 m

3. Results

3.1 Grid Independence Test (GIT)

A grid independence test (GIT) was conducted to determine a suitable number of nodes for the model. The mesh of the model was constructed using different element sizes. This gives different numbers of elements and nodes. In this study, the velocity profile was used to identify suitable numbers of nodes for use in the tumor model. five different element sizes were created. The number of produced nodes was 2,9513-4,32803 (Figure 4). This figure shows that the number of nodes within 222, 822 and 328,011 has a suitable number of nodes to serve as a reference for the remaining model ehich an element size with a low percentage error was used as a reference.

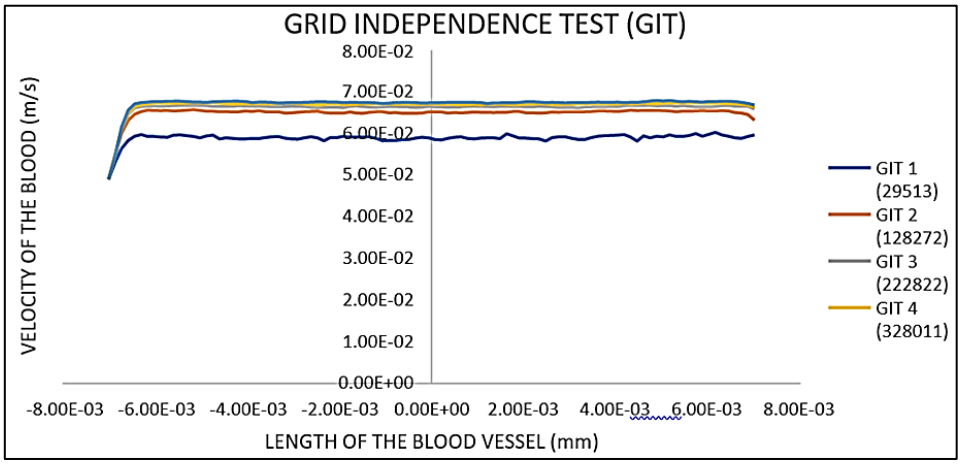

Fig. 4. Velocity profile for different nodes number for GIT

3.2 Temperature Distribution in Tumor Tissue

3.2.1 Temperature of 40°C

When the inlet heat was 40°C, the results showed that the heat propagation differed for different sizes of the model (see Figure 5).

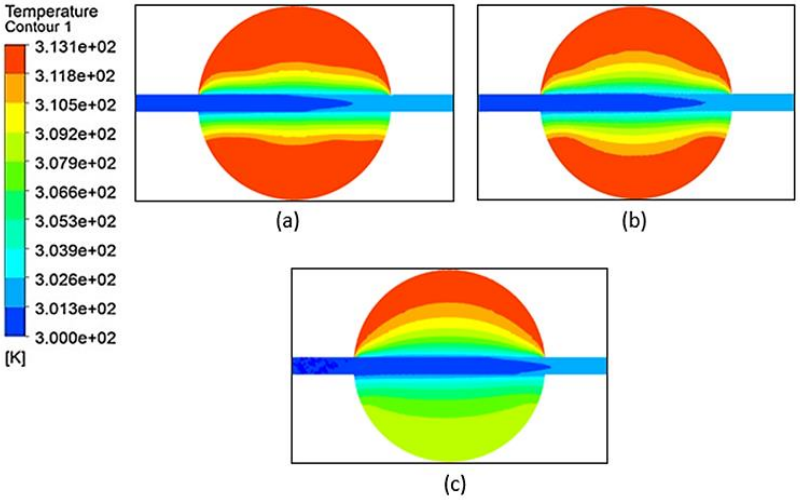

Fig. 5. Temperature distributions in the tumor model at 40 ℃ (a) A =4 mm (b) B=3 mm (c) C=2 mm

Based on the results, it can be concluded that the radiation on the model affected not only the tumor tissue but also the blood vessels. As the model size increased, the temperature on the right side of the blood vessel decreased. It can be the area covered by the higher temperature in the contour and in Figure 6. In Models A and B, there is also an area with high temperature on the lower side of the model. Meanwhile, for Model C, the temperature on the lower side was not as high as that of the other models. The figure shows the changes in tumour tissue and blood vessels. The starting point was the tumour surface.

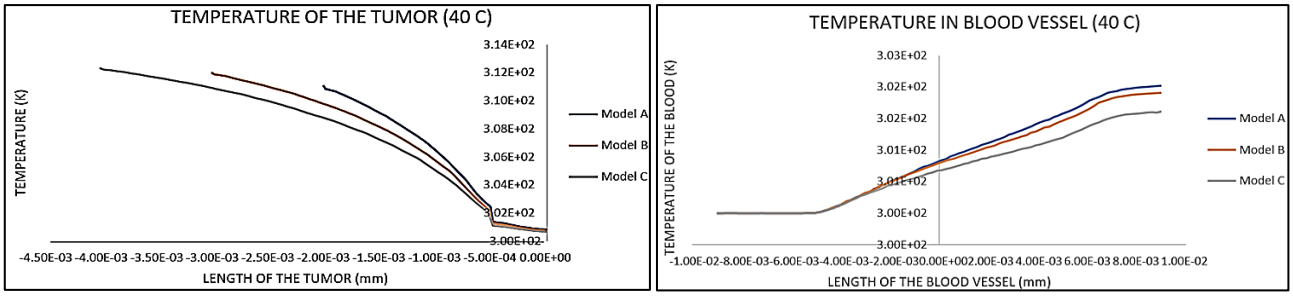

(a) (b)

Fig. 6. Temperature profile (a) Tumor tissue (b) Blood vessel

3.2.2 Temperature of 42.5°C

As shown in Figure 7, the area of high heat increased on the upper side of the tumour. On the lower side of the tissue, models A and B had temperatures similar to 40°C. Figure 8 presents the graph temperature of tumour and blood vessel.

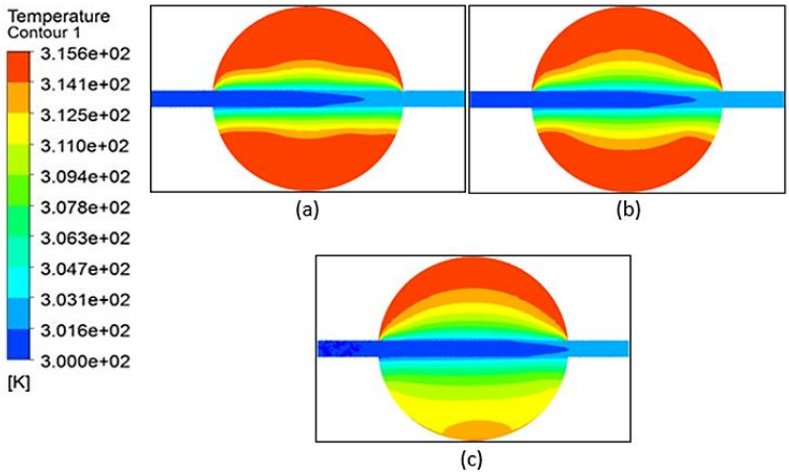

Fig. 7. Temperature distribution of the tumour model at 42.5℃ (a) A=4 mm (b) B=3 mm (c) C=2 mm

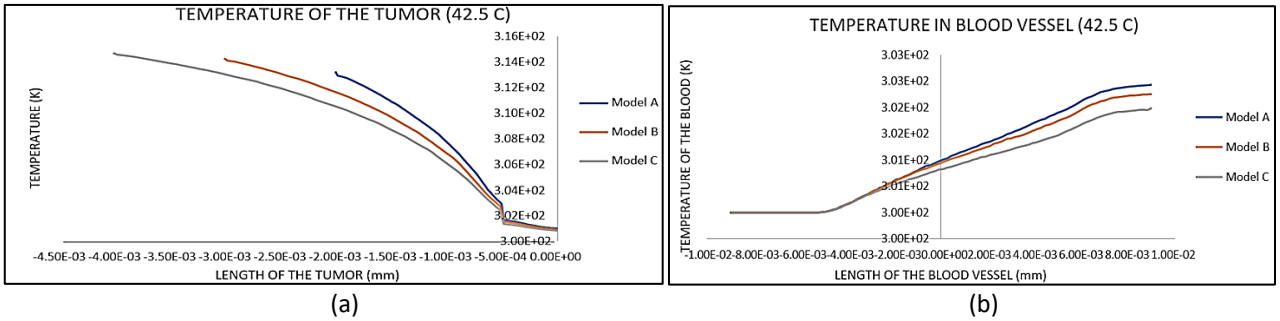

(a) (b)

Fig. 8. Temperature profile (a) Tumor tissue (b) Blood vessel

3.2.3 Temperature of 45°C

The results were not significantly different from those obtained at 42.5°C. The contour of the heat propagation was the same as that of the previous case, as shown in Figure 9. The difference is that the size of the higher-temperature area increased. When taking a closer look, the area with higher blood vessel temperatures also became wider than the temperature of radiation increased. The graph in Figure 10 shows that the temperature increased at certain parts of the model.

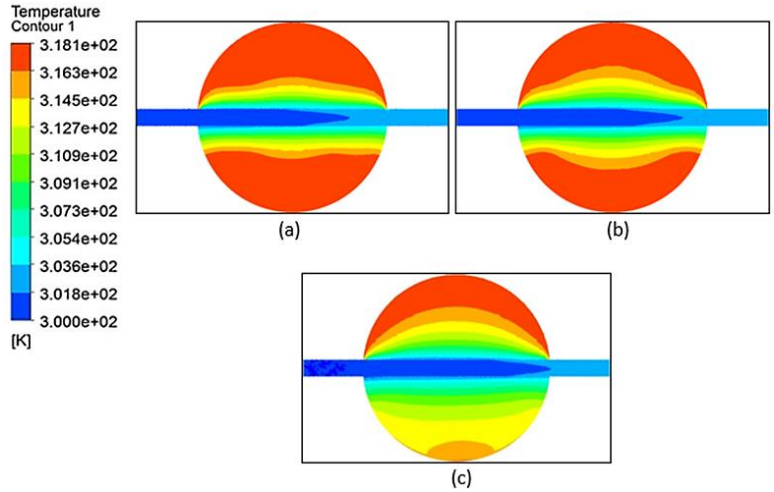

Fig. 9. Temperature distributions of the tumour model (a) A =4 mm (b) B=3 mm (c) C=2 mm

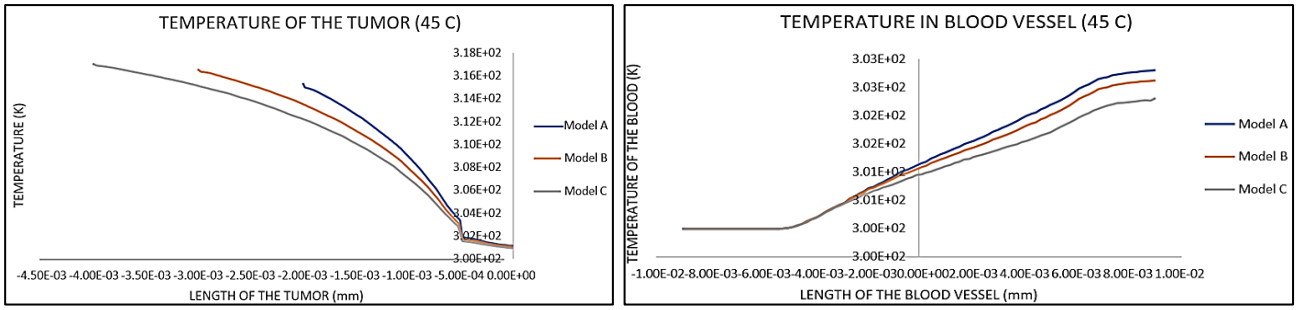

(a) (b)

Fig. 10. Temperature profile (a) Tumor tissue (b) Blood vessel

3.3 Velocity of Blood

It is important to know how heat radiation affects blood velocity. Tissue size is also a major cause of blood velocity differences.This is because as the tissue size increases, the amount of heat required to reach the blood will be limited, as shown in the temperature contour. Because the radiation temperature in this study also varied, the outlet velocity could differ in each case. In this case, the inlet velocity was constant for all tested cases and models (0.049 m/s). The data from the simulation were exported to obtain blood vessel velocity.

3.3.1 Velocity at 40°C

Because the data were read along the axis, the length of the blood vessel was started from a negative value. From the plotted graph in Figure 11, it can be seen that the velocity increased at the beginning for each model. However, after the rapid increase, the velocity started to remain constant with a small fluctuation along the blood vessel. At the end of the graph, the velocity exhibits a small decrease. The graph also shows that all models have similar patterns, and the values vary slightly.

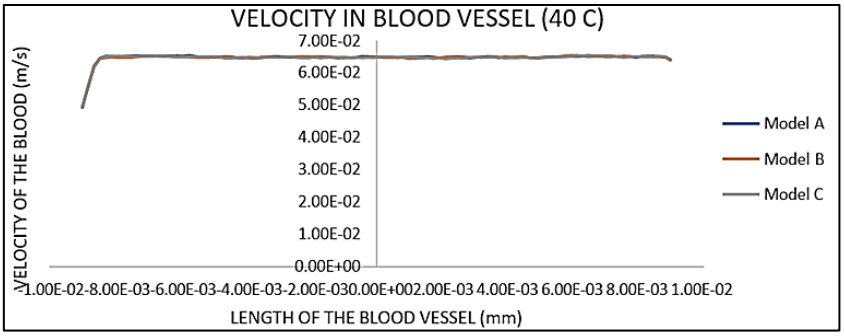

Fig. 11. Profile of blood velocity at 40°C

3.3.2 Velocity at 42.5°C

For this case, the results obtained for the blood vessel is same like 40°C, as illustrated in Figure 12. This finding is possibly attributable to the result obtained at the center of the blood vessel, which did not differ significantly from previous cases because heat propagation was not significantly affected by increasing the radiation temperature. Additionally, the shape of the blood vessel wall, which was a simple cylinder, caused the result to remain constant.

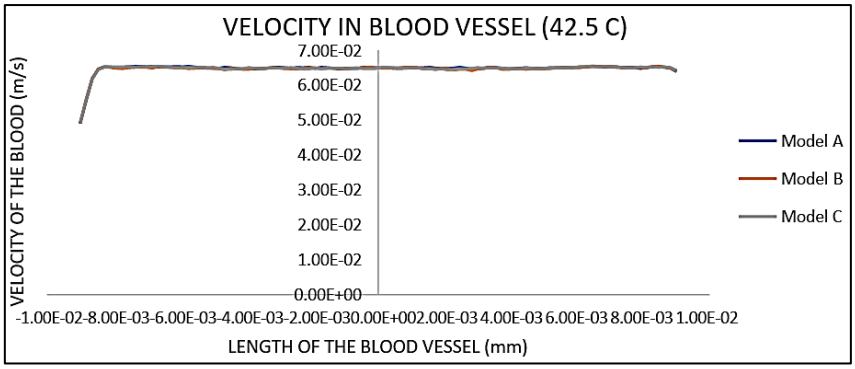

Fig. 12. Graph of blood vessel velocity at 42.5°C

3.3.3 Velocity at 45°C

Like the other cases, the results for the velocity at 45°C temperature is still same with the previous case presented in Figure 13. This indicates that different radiation temperatures did not affect much toward the blood vessel. However, this may be due to the configuration that was set before the simulation was performed. This figure proves that the result is similar to the results for the velocity at 40°C and 42.5°C.

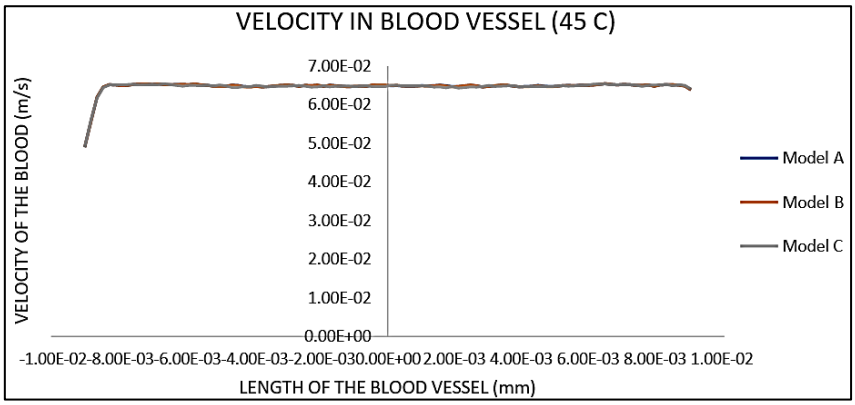

Fig. 13. Graph of blood vessel velocity at 45°C

3.4 Pressure Distribution in the Blood Vessel

As heat is applied to the model, the other element that needs to be observed is the pressure distribution in the model. Pressure may not have a significant effect on the tumour model, but it is important to determine how heat propagation impacts this value. For the setup, the pressure is set 0 Pascal at the outlet of the heat source and blood vessel.

From the observation, the distribution of the pressure in the tumor tissue is constant. Additional a pressure distribution can be observed at the blood vessel. At the inlet of the blood vessel, the pressure was the highest. As it flows toward the outlet, the pressure decreases, as shown in Figure 14. At the outlet of the blood vessel, the pressure is 0 Pascal, which is set in the setup. The results for pressure at 40°C, 42.5°C, and 45°C are the similar.

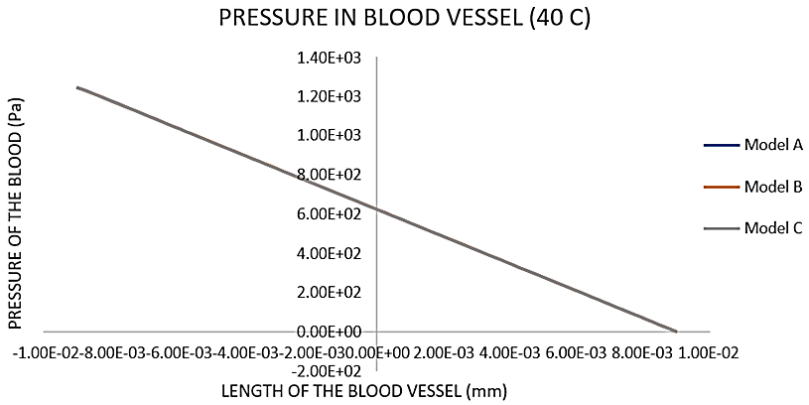

Fig. 14. Pressure profile of blood vessel

4. Conclusions

The results show that radiation can affect blood vessels. The contour of the model differs for each case. Model C had a higher temperature, indicating that heat can penetrate deeper when the tumour is large. However, the blood vessel temperature of model A was the highest among the others. This may be due to radiation exposure when the tumour is small. In addition, the velocity results for each case is the same. The same thing happens for the pressure result, where all cases have similar results.

This study has achieved the objective of determining the temperature distribution of malignant tumors of different sizes. The temperature contours indicate that malignant tumors of different sizes have different temperature distributions. Finally, this study fulfills another objective: heat penetration from an infrared source, from which data on temperature at a certain depth for malignant tumors can be obtained.

Acknowledgement

This research was supported by Universiti Tun Hussein Onn Malaysia (UTHM) through MDR (vot Q686).

References

[1] Mattiuzzi, Camilla, and Giuseppe Lippi. "Current cancer epidemiology." *Journal of Epidemiology and Global Health* 9, no. 4 (2019): 217-222. https://doi.org/10.2991/jegh.k.191008.001

[2] Bland, Kirby I., Edward M. Copeland, V. Suzanne Klimberg, and William J. Gradishar. *The breast: comprehensive management of benign and malignant diseases*. Elsevier Health Sciences, 2023.

[3] Sontheimer-Phelps, Alexandra, Bryan A. Hassell, and Donald E. Ingber. "Modelling cancer in microfluidic human organs-on-chips." *Nature Reviews Cancer* 19, no. 2 (2019): 65-81. https://doi.org/10.1038/s41568-018-0104-6

[4] Klein, Christoph A. "Cancer progression and the invisible phase of metastatic colonization." *Nature Reviews Cancer* 20, no. 11 (2020): 681-694. https://doi.org/10.1038/s41568-020-00300-6

[5] Follain, Gautier, David Herrmann, Sébastien Harlepp, Vincent Hyenne, Naël Osmani, Sean C. Warren, Paul Timpson, and Jacky G. Goetz. "Fluids and their mechanics in tumour transit: shaping metastasis." *Nature Reviews Cancer* 20, no. 2 (2020): 107-124. https://doi.org/10.1038/s41568-019-0221-x

[6] Hisada, Yohei, and Nigel Mackman. "Tissue factor and cancer: regulation, tumor growth, and metastasis." In *Seminars in Thrombosis and Hemostasis* 45, no. 4 (2019): 385-395. https://doi.org/10.1055/s-0039-1687894

[7] Debela, Dejene Tolossa, Seke GY Muzazu, Kidist Digamo Heraro, Maureen Tayamika Ndalama, Betelhiem Woldemedhin Mesele, Dagimawi Chilot Haile, Sophia Khalayi Kitui, and Tsegahun Manyazewal. "New approaches and procedures for cancer treatment: Current perspectives." *SAGE Open Medicine* 9 (2021): 20503121211034366. https://doi.org/10.1177/20503121211034366

[8] Zhang, Min, Mao-Sheng Cao, Jin-Cheng Shu, Wen-Qiang Cao, Lin Li, and Jie Yuan. "Electromagnetic absorber converting radiation for multifunction." *Materials Science and Engineering: R: Reports* 145 (2021): 100627. https://doi.org/10.1016/j.mser.2021.100627

[9] Kane, Suzanne Amador, and Boris A. Gelman. *Introduction to physics in modern medicine*. CRC press, 2020. https://doi.org/10.1201/9781315232089
[10] Malviya, Rishabha, Dhanalekshmi Unnikrishnan Meenakshi, and Priyanshi Goyal, eds. "Laser therapy in healthcare: Advances in diagnosis and treatment." Wiley, (2024). https://doi.org/10.1002/9781394237999
[11] Chen, Xiaofeng, Jibin Song, Xiaoyuan Chen, and Huanghao Yang. "X-ray-activated nanosystems for theranostic applications." *Chemical Society Reviews* 48, no. 11 (2019): 3073-3101. https://doi.org/10.1039/C8CS00921J
[12] ha, Sheetal, Pramod Kumar Sharma, and Rishabha Malviya. "Hyperthermia: Role and risk factor for cancer treatment." *Achievements in the Life Sciences* 10, no. 2 (2016): 161-167. https://doi.org/10.1016/j.als.2016.11.004
[13] Kok, H. Petra, and Johannes Crezee. "Hyperthermia treatment planning: clinical application and ongoing developments." *IEEE Journal of Electromagnetics, RF and Microwaves in Medicine and Biology* 5, no. 3 (2020): 214-222. https://doi.org/10.1109/JERM.2020.3032838
[14] Cheng, Yi, Shanshan Weng, Linzhen Yu, Ning Zhu, Mengyuan Yang, and Ying Yuan. "The role of hyperthermia in the multidisciplinary treatment of malignant tumors." *Integrative Cancer Therapies* 18 (2019): 1534735419876345. https://doi.org/10.1177/1534735419876345
[15] Lee, Donald H., Jeffrey M. Hills, Martin I. Jordanov, and Kenneth A. Jaffe. "Common tumors and tumor-like lesions of the shoulder." *JAAOS-Journal of the American Academy of Orthopaedic Surgeons* 27, no. 7 (2019): 236-245. https://doi.org/10.5435/JAAOS-D-17-00449
[16] Sinha, Shantanu, and Usha Sinha. "Functional magnetic resonance of human breast tumors: diffusion and perfusion imaging." *Annals of the New York Academy of Sciences* 980, no. 1 (2002): 95-115. https://doi.org/10.1111/j.1749-6632.2002.tb04891.x
[17] Ara, Sharmin, Annesha Das, and Ashim Dey. "Malignant and benign breast cancer classification using machine learning algorithms." In *2021 International Conference on Artificial Intelligence (ICAI)*, p. 97-101. IEEE, 2021. https://doi.org/10.1109/ICAI52203.2021.9445249
[18] Khairunnahar, Laila, Mohammad Abdul Hasib, Razib Hasan Bin Rezanur, Mohammad Rakibul Islam, and Md Kamal Hosain. "Classification of malignant and benign tissue with logistic regression." *Informatics in Medicine Unlocked* 16 (2019): 100189. https://doi.org/10.1016/j.imu.2019.100189
[19] Lüönd, Fabiana, Stefanie Tiede, and Gerhard Christofori. "Breast cancer as an example of tumour heterogeneity and tumour cell plasticity during malignant progression." *British Journal of Cancer* 125, no. 2 (2021): 164-175. https://doi.org/10.1038/s41416-021-01328-7
[20] Chanmugam, Arjun, Akanksha Bhargava, and Cila Herman. "Heat transfer model and quantitative analysis of deep tissue injury." In *ASME International Mechanical Engineering Congress and Exposition*, 45189, p. 717-723. 2012. https://doi.org/10.1115/IMECE2012-88405